CFD-URANS ANALYSIS OF THE WATER FLOW IN AN ALGAE MAGNETIC SEPARATOR

by

Shreyas Sahadev Joshi

A thesis submitted to the faculty of
The University of North Carolina at Charlotte
in partial fulfillment of the requirements
for the degree of Master of Science in
Mechanical Engineering

Charlotte

2018

Approved by:

_____
Dr. Navid Goudarzi

_____
Dr. Russel Keanini

_____
Dr. Mesbah Uddin

ABSTRACT

SHREYAS SAHADEV JOSHI. CFD-URANS ANALYSIS OF THE WATER FLOW IN AN ALGAE MAGNETIC SEPARATOR (Under the direction of Dr. Navid Goudarzi)

Crude oil is one of the major sources for energy production. One barrel could produce up to 50% of gasoline. Almost, 75% of a crude oil barrel can be converted to petroleum products which are the most consumable energy sources over the world. With increase in the energy demand and limited sources of crude oil, it is necessary to acquire new sources for energy production. There has been an increasing interest in biofuel as a source of energy since past decades. Using algae for biofuel production has been drawing more attention in recent years. Literature shows the complications involved in the commercialization of the algae-based biocrude. Among different processes involved in biocrude production, harvesting is one of the most time and cost consuming steps that require further development to obtain more efficient and cost-effective solutions. This MSc thesis research is focused on solving three-dimensional unsteady and steady Navier-Stokes equations numerically to investigate the turbulent flow field going through an open channel algae magnetic separator. The numerical simulation is conducted in StarCCM+, a computational fluid dynamics (CFD) software. An Eulerian multiphase flow model, volume of fluid (VOF) model, is applied to determine to track the shape and position of the interface. Different eddy-viscosity turbulence models such as $k-\varepsilon$ and SST $k-\omega$ are used to predict the unsteady velocity fluctuations along the algae separator. The grid analysis is conducted to determine the appropriate mesh resolution. The results indicated that using VOF approach using RANS turbulence model and well-resolved grids on the

walls obtain a reliable predictive tool for analyzing the flow field going through the studied system. However, validation of the results is required using experimental analysis. The results also established recommendations for improving the design geometry of the algae magnetic separator.

ACKNOWLEDGMENTS

My special thanks go to my advisor Dr. Navid Goudarzi, for his support and guidance throughout my research work. Especially, I would like to express thanks for his patience for the project conducted parallel to the work presented in this thesis. I would like to thank Manta Biofuel, LLC for making available this research opportunity. It would not have been successful without their support to complete this work. I appreciate my committee members, Dr. Russell Keanini and Dr. Mesbah Uddin for their valuable time going through my work and guidance for this research. I would also like to thank all my fellow colleagues in graduate school: Saisri Aditya Kanchibhotla, Dheeraj Muthyala, Sridhar Dangeti and Srivatsa Mallapragada for sharing their moments in my study. I would like to extend my thanks to all faculty and staff members of the Department of Mechanical Engineering and Faculty of Graduate Studies, and not to forget all my friends for their help. At last, I would like to thank UNC Charlotte's facilities without which this work was not possible.

DEDICATIONS

To my parents

Mr. Sahadev Bhikaji Joshi and Mrs. Snehal Sahadev Joshi

My beloved sister

Siddhita Sahadev Joshi

&

My brotherly friend

Pramod Gaikwad

TABLE OF CONTENTS

LIST OF TABLES

LIST OF FIGURES

NOMENCLATURE

GENERAL FLUID MECHANICS

I	Identity tensor
S	Mean strain rate tensor
T	Turbulent time scale
k	Kinetic energy
q	Heat flux
v	Continuum velocity
C_{ε_1},C_{ε_2} C_{ε_3}	Model coefficient
C_{μ}	Model coefficient
D_{ω}	Cross-derivative term
G_b	Turbulent production due to buoyancy
G_k	Turbulent production
G_{nl}	Non-linear production term
G_{ω}	Production of specific dissipation rate
S_E	Energy source per unit volume

S_k , S_ε	User-specified source terms
S_ω	User-specified source term
T_t	Reynolds stress tensor
Y_M	Dilatation dissipation
f_b	Resultant body forces
f_c	curvature correction factor
f_{β^*}	Free shear modification factor
f_μ	Damping function
v_g	Reference frame velocity
$\bar{v}$	Mean velocity
β	Model Coefficient
ε	Turbulent dissipation rate
μ	Dynamic viscosity
ν	Kinematic viscosity
ρ	Density
σ	Stress tensor

ω	Specific dissipation rate
γ', γ_{trans}	Transition model
μ_t	Turbulent viscosity
σ_k ,σ_ε	Turbulence Schmidt numbers
σ_ω	Inverse turbulence Schmidt number

LIST OF ABBREVIATIONS

CAD	Computer-Aided-Design
CFD	Computational Fluid Dynamics
DEAE	DiEthyl AminoEthyl
EIA	U.S. Energy Information Administration
HTL	HydroThermal Liquefaction
PEI	Polyethylenimine
RANS	Reynolds Averaged Navier Stokes equation
RST	Reynolds Stress Tensor
VOF	Volume of Fluid

Chapter 1. A VISION TO NEW SOURCE OF ENGERGY PRODUCTION

Crude oil is a major source of production of petroleum products. Vehicles working on the fossil fuels require crude oil for their production. Around 50% of a barrel can be converted to gasoline [1]. U.S. Energy Information Administration (EIA) has forecasted increase in the price of crude oil by $3 by 2018 due to increase in demand [2]. Crude oil is essentially composed of hydrocarbon deposits and other organic materials. It is a type of naturally occurring fossil fuel that can be refined to produce various petroleum products such as gasoline, diesel and various forms of petrochemicals. Although, it is a prime source of energy, one need not to forget that it is a non-renewable source which can't be replaced. Current increase in demand and scant of the crude oil sources could become an impediment to the moving world. This lead to move towards more ecological and renewable source of energy which could succor to withstand the world's energy demand in near future. While technologies using green energy resources are emerging in recent years, many of industrial applications still rely on conventional energy resources. This requires the same or higher production of conventional energy resources. An alternative green solution to address the current and future energy demand, is to exploring other energy production practices. In fact, various environmental and hazardous issues are concerned with the conventional production of these sources.

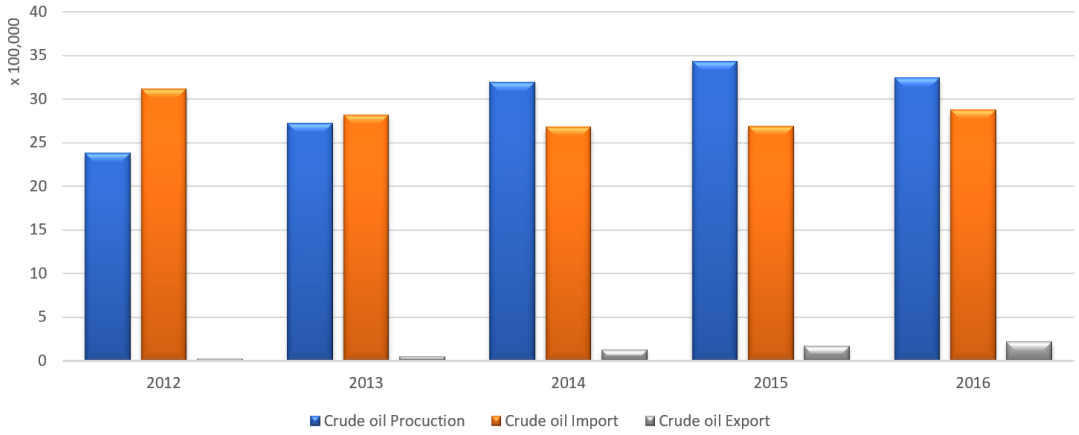

Figure 1 EIA Crude Oil Statistical data for the year 2012 to 2016

Crude oil exploration process requires drilling for oil, affects both marine and land ecosystem in large scale [3]. Technologies like satellites, global positioning systems, remote sensing devices, and 3-D and 4-D seismic technologies assist to discover the oil reserves while scaling down the affected area by drilling fewer exploratory wells. Mobile and smaller slim-hole drilling rigs reduced the size of the area that drilling activities affects. Further, the use of horizontal and directional drilling made possible for a single well to acquire oil from a larger area which reduced the required number of extracting wells to develop an oil resource.

Although, attempts have been made with new technologies to scale down the affected area, still it affects the environment where these extraction processes are carried out. Apart from these, history is evident of the fact of oil spills caused damage not only to the scant source of energy with around millions of wasted barrels but to the environment as well [Figure 2].

Figure 2 [Left] Around 206 million gallons Burnt in Mexico Gulf during oil spill[4].[Right] The pipeline leaked more than 200,000 gallons of oil in South Dakota[5]

Biofuel production using algae has recently drawn more interest amongst researchers to improve the quality and production rate of the produced biofuel and to commercialize it as a green energy source. Biofuel-based power production has certain benefits. One of the major benefits is that algae exists everywhere in the biosphere making them largely available source of energy. Micro algae can fix global carbon content more than 40% through efficient utilization of carbon dioxide [6]. These makes them very suitable as a renewable source for production of crude oil. It has plant like functions such as photosynthesis without true developed roots, stem, leaves, flowers and vascular system [7]. Algae has limited applications such as agar, alginates, energy feedstock, fertilizer, nutrition, pollution bioremediation, natural pigments (carotenoids and - chlorophylls) and stabilizing substances[8]. In biotechnology industry, algae are used for the extraction of glycerol, enzyme and other relevant products [9]. Algae received its prominence in biofuel due to plentiful availability of pigments (i.e. lipid, fatty acid and carbohydrate) and possesses biosorption ability [10, 11]. Golueke et al. [12] were the first to provide biomass application to produce biomethane gas using anaerobic digestion process.

Demirbas, A. and M.F. Demirbas [13] reported that algae can produce 20,000-80,000 liters of oil per acre of algal crops which is 30 times higher than oil produced from crops such as palm oil. P. Vo Hoang Nhat et al. [14] in their recent research on assessing algae to use as green process for

biofuel production in future thoroughly considered the latest technologies involved in cultivation of algae and production of biofuel. In their study, they observed with optimization and combinations of other chemical and biological processes could lead to bio oil yield up to 41.1%. They also mentioned a life cycle assessment of algae that could achieve high energy return than fossil fuels and can be considered as green approach for biofuel production. However, the price of biofuel is higher than fossil fuel by approximately $1/liter and hence making it expensive fuel. Ruiz et al. [15] admitted that algae-based biofuel could not produce immediate large revenues but believed in coming decade trend will change due to improvements in biotechnology. Gambelli et al. [16] forecasted that it will become acceptable and dominate around 75% of the market by the year 2030.

Chapter 2. ALGAL BIOMASS CONVERSION: AN ECONOMIC HURDLE

Converting algal biomass requires plentiful attention on many levels of biotechnology. Many hurdles come at first stage from the production of biomass itself. Numerous issues are involved in every step of production process. This chapter deals with the whole production process of algal biomass conversion into biofuel with various methods involved and their respective challenges in implementation.

LIPID CONCENTRATION

Lipid concentration in algae biomass is one of the main factor for biofuel production. Numerous significant attempts have been focused on improving lipid concentration during cultivation. During normal cultivation methods lipid accumulation is low and hence to improve lipid content various methods such as cultivation in nutrient imitation/starvation, use of mixed culture, reactor design (open pond, closed photobioreactor, etc.) and supplementation of chemicals and hormones etc. are used. The nutrient (nitrogen) limitation has shown better results which lead to use it widely. Oil productivity from microalgae can reach 100 times higher than agricultural crops used for oil production such as soy, palm and canola [7, 17]. The most common microalgae used for biodiesel production belongs to *Chlorella, Dunaliella, Nannochloris, Nannochloropsis, Neochloris, Porphyridium,* and *Scenedesmus fgenera* which contains 20-50% of lipids by weight [7]. Also, bio-oil yield depends on the type of algae and their composition. The bio-oil yield can be enhanced by growing right algae which indicated by Singh [18] using three different samples of macro algae where the maximum bio-oil yield of *Ulva fasciata* was recorded as 12% and lowest of 7% was produced by *Enteromorpha sp*. However, it was evident from the fact that macro algae had comparatively lesser lipid concentration than microalgae which made microalgae to provide enhanced bio-oil yield.

CULTIVATION PROCESS:

Algae cultivation does not require much of farming expertise and requires mainly sunlight to grow. Their growth period is comparatively small and does not require very special habitat to grow. In fact, it can grow in unfavorable condition to most of the plants. Also, higher the concentration of algae cells, reduces the ability to absorb the light. In such conditions called heterotrophic, instead depending on the light it use other carbon sources such as sugars, organic acids, and other organic carbons as carbon sources.

Although, algae can grow in most adverse conditions, but considering from commercializing it as a source to produce biofuel could require special attention to be provided to enhance their growth scale. As mentioned earlier cultivation methods can improve the lipid content. Applying right cultivation method not only could enhance the production of biofuel but also reduce the cost of production. Hence selection of suitable cultivation system is a prime factor at early stage of production process. Selection of cultivation system should be based on biomass production and lipid productivity. The other important factors involve nutrition supply factors such as gas transfer, mixing and light requirement [19]. As some of cultivation methods are expensive making scalability as one of the limiting factor in the cultivation process that could directly affect commercialization of the biofuel.

Following are the cultivation methods most commonly used:

- Suspended cultivation
- Attached Cultivation

In suspended cultivation, most affordable way to cultivate is use of open pond system. It incorporates shallow channels like raceways equipped with paddle wheel to mix the suspension [20]. In this method, nutrients and microalgae are circulated continuously. This system is widely

used over 90% in the world [21]. Theoretically, biomass productivity is within the range of 50-60 g/m^2/d. However, according to Shen et al. [22], even 10-20 g/m^2/d is not practically possible. Closed photobioreactor method considers various factors to overcome inefficiencies involved in open pond systems and outperform them but are relatively costly [7, 23]. This method utilizes closed systems made from transparent tubes, plates, bags or hemispherical dome [24] and allows mixing, temperature and CO_2 supply controls. More in detail about various types of system is provided by Shukla et al. [25].

Attached culture provides a better solution to cultivation method due to advantages involved such as high cell density, lower water and land requirement which made this new method a growing interest [26-28]. This method classified into two types namely matrix- immobilized system and biofilm system. In this method, bio film is formed by growing algal cells on surface of a material. Compared to suspended cultivation system, this method offers higher biomass yields and easy to scale up with better light distribution within the reactor and better control of contamination [28].

PRODUCTION PROCESS OF BIOFUEL:

Algae biomass can be converted to liquid biofuels by following three main routes namely extraction or transesterification (biodiesel), bio-oil via pyrolysis, and biocrude via hydrothermal liquefaction (HTL) [29]. HTL process is used for biocrude production that requires less energy and has advantages over other methods. This process is selected for further elaboration here. However, Mathur et al. [30] has provided in detail description of various biofuel conversion methods in their research. Main approaches of the production of biofuel is shown in Figure 3.

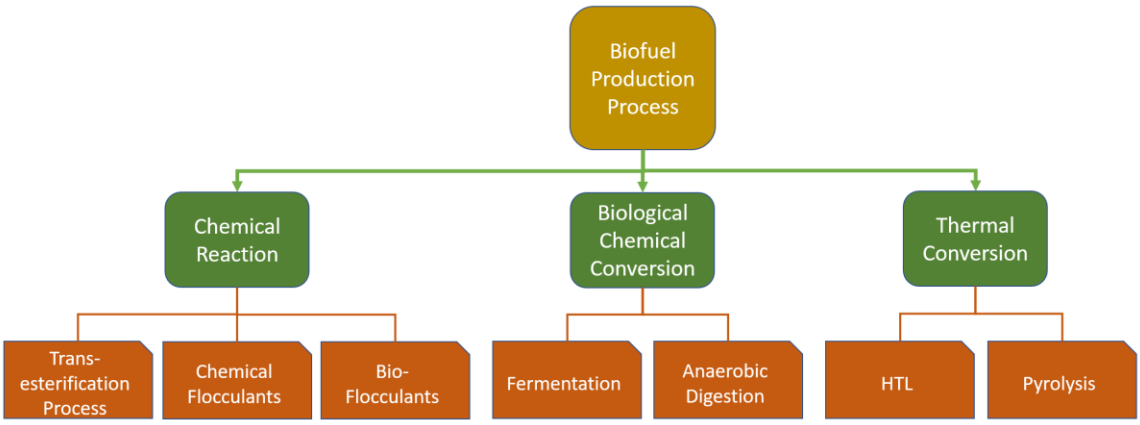

Figure 3 Conversion methods of Algae to biofuel

Hydrothermal liquefaction (HTL) process:

It is a direct liquefaction process, producing bio-oil in the relative oxygen absence state by pressurizing inert gases such as N2 or He or reducing gases such as H2 or CO at high temperatures in the range of 200–380 °C with pressure of 5–28 MPa. This method has substantial advantages compared to the traditional bio-oil production methods due to rapid reaction, use of high moisture content feedstock with no lipid content restriction i.e. all organic components of algal biomass not limited to lipids can be converted into biocrude [31]. Also, HTL process does not require intensive amount of energy for drying stages [32]. Further enhancements in this process using microwave assisted heating is provided by Reddy et al. [33] put new insight against conventional heating in which showed capability of complete extraction of the lipid content. According to several authors temperature and catalysts are the prime factors in optimization of HTL process for enhanced bio-oil production [34]. Tommaso et al. [35] proposed reuse of aqueous phase of HTL process for anaerobic degradation and Maddi et al. [36] suggested for chemical and liquid fuel production. Shanmugam et al. [37] use struvite formation and able to recover 99% phosphorus and 40–100% ammonia which could be recirculated to the algae cultivation process to make it more economical. These researches showed the importance of aqueous phase in HTL process and can be improved to

reduce the overall cost of production of bio-oil. In depth detail of HTL process along with challenges to incorporate this process is given by Tien et al. [38].

HTL and Pyrolysis both could produce similar quality and yield of biofuel. However, with carbon chains of C_4 to C_{20} can be obtained using pyrolysis process and HTL was better used for the production of C_4 to C_{22} carbon chains, including major of C_6, C_{16} and C_{18} [39]. Liu et al. [40] showed through life cycle assessment process that algae bio-energy generating from HTL process result in high energy return than petroleum fuel. Cerón et al. [41] and Roesijadi et al. [42] compared HTL process with transesterification and fermentation process respectively and found HTL was providing better revenue. The identity of algae feedstock is the most important criterion in bio-energy production as it could affect employed method's efficiency of production.

HARVESTING METHODS:

Harvesting is a critical step in the bio-oil production process to aggregate the biomass for producing bio oil. Microalgae cells are generally in size of 1-20 μm that makes them very difficult to harvest [43, 44]. Also, density of the fresh water microalgae ranges between 1040- 1140 kg/m^3 [45, 46] and according to Granados et al. [47], densities of fresh and salt water is almost similar that makes the rate of settlement of the algae vary low. This identical densities involved of the cells and media makes algae harvesting very difficult to achieve [48]. Studies shown that in the collide of alga and water, algae possess very high zeta potential making it a stable suspension in aqueous medium. Hence, make it difficult to sperate with the help of sole gravity under natural conditions. It was found that around 40% cost of production constitutes for the cultivation and more than 60% cost of production constitutes for the biomass harvesting making biofuel production expensive [49]. According to Udom et al. [50], in biodiesel production the cost of harvesting constitutes 2-60% of the production. Therefore, it is required to educate with comparative knowledge of existing

methods and respective achieved advancements before attempting to optimize for the critical conditions to obtain maximum biomass recovery. According to Shelef et al. [51], to choose right method one should identify algal species, growth medium, and end product in the biofuel production. Comparative study of the various harvesting methods is provided by Uduman et al. [52]; Zhou et al. [53]; Debora and Edward [54] in their researches. Main categories of the harvesting methods are shown in Figure 4.

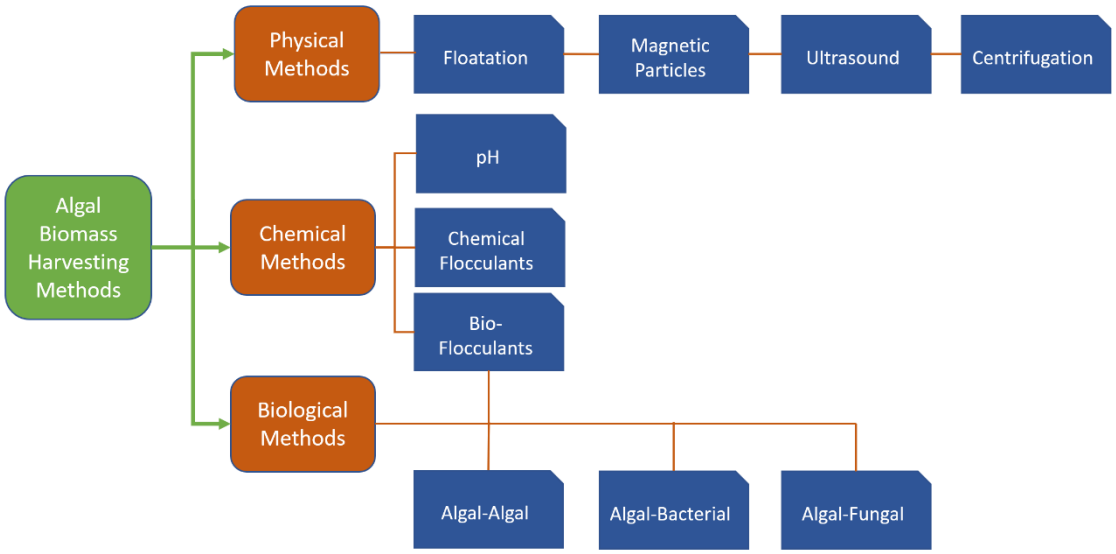

Figure 4 Various methods used for algal harvesting

Through advancement in biotechnology numerous systems have improved. Amongst various methods, magnetic particles method was observed cheaper and low energy consuming, therefore, only this method is provided in brief. In depth details of various harvesting methods is provided by Mathur et al. [30]. Most of the current technologies are not that efficient and/or costly which is a hindrance for commercialization of the biofuel. Some of the costing and their respective efficiencies is mentioned in Table 1.

Table 1 Some aspects of the harvesting processes in practice

Method	Advantage	Disadvantage
Filtration	Cost effective	Slow, membrane fouling, cell damage
Floatation	Low cost	Very slow, less efficient
Centrifugation	Fast, efficient	High energy intensive, large scale issues
Gravity Sedimentation	Low cost, low energy requirement	Slow, require high cell density
Chemical Flocculation	Low cost, low cell damage, highly efficient	Possible risk of degrading the biomass quality and yield
Dissolve air Floatation	Low cost, easy upgrade to pilot scale	Energy intensive, possibility of product quality degradation
Bio – Flocculation	Highly efficient	High energy requirement than other flocculants
Electrolytic flocculation	Highly efficient	High energy requirement, electrode fouling, high system temperature
Submerged membrane filtration	Low cost, less shear to cells	Membrane fouling
pH	Large scale, efficient up to 80-90%	Corrosive leading to poor performance (NaOH and KOH)
Ultrasound	Highly efficient up to 93%, no fouling, long lasting, less tendency of mechanical failure	High energy requirement

MAGNETIC PARTICLES:

This technique is easy and cheaper with quick separation and low energy consumption, where many researchers are working to optimize it [55, 56]. In this technique, algal cells get absorbed on magnetic particles (in the form of precipitated magnetite, silica coated hydrophilic magnetic particles [57] and surface modified magnetic beads with *diethyl aminoethyl* (DEAE) and *polyethylenimine* (PEI) [58] due to electrostatic forces [56]. Their separation largely depends on magnetic beads, algae concentration and pH. Cerff et al. [57] proposed a new basis to this technology as zeta potential and concluded these magnetic particles might show ion exchange capability to the cells. In recent advancement, ferric nanoparticles (Fe_3O_4) were used in which electrostatic interaction between positively charged nanoparticles attracted the negatively charged algal cells. In the assessment of the magnetic particle method, various microalgae were used such as *Botryococcus braunii, Chlorella ellipsoidea* [56], and *Nannochloropsis maritime* [55]. In these researches, increase in aggregation of algal cells at neutral or alkaline pH with high efficiency at

low dosage of alkaline pH was found which was measured in terms of hydraulic diameter of algal-nanoparticle complex. This method showed very high recovery efficiency rate up to 95 -97% within time period of 4 -5 min [30]. Further, recovery and reuse of liquid nutrient media for cultivation [55]and magnetic nanoparticles [56] after separation was observed up to 5 cycles. Figure 5 represents a magnetic separator system for algae harvesting developed be Hu et al. [59]. It incorporates a chamber, a magnetic drum, a scraper blade, an inlet and two outlet ports. Wang, Shi-Kai et. al. [60] reviewed the magnetic separator system; the review includes the overall system process and various biological and chemical factors affecting the performance of the system. The majority of the existing literature focus is on optimizing the system with focus on a synthesis of efficient magnetic reagents, separation process, the detachment of the particle-cell aggregates, low energy consumption, reusability of medium, and magnetic particles. This MS thesis provides a basis for studying the fluid flow behavior in the algae harvesting systems and understanding the complications involved in harvesting process based on fluid analysis.

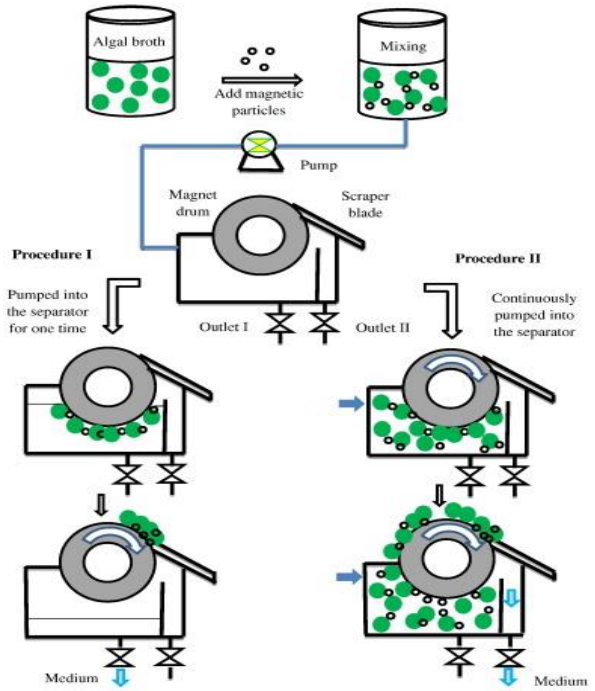

Figure 5 Schematic representation of the magnetic algae separator[60]

To sum up, renewable crude oil generation process takes place in three steps [Figure 6] as follows:

- Grow Algae
- Harvest Algae
- Convert algae into crude oil

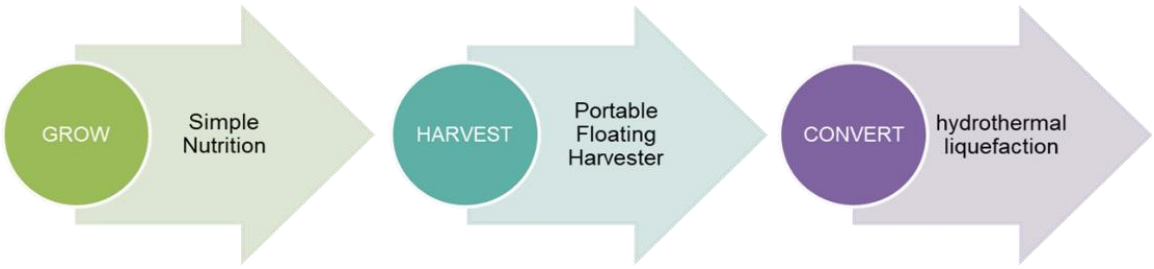

Figure 6 General Biocrude oil production process

Numerous research has taken interest in algae cultivation and improving Algae bioreactor performance using Computational Fluid Dynamic (CFD) analysis since 2005. It has shown great increased interest in producing biofuel from algae since last decade and constantly improvement has been notified by many researchers. Main concern which is mentioned in this research is harvesting these algae out of the river or pond as quickly as possible. Hastening this process requires significant attention on the algae harvesting systems performance. The other main concern of the system is cost of production and portability. This renewable generation process to make it economical requires this system to be cheaper than the currently present harvesters and yet efficient [Table 1]. To achieve this, it is required to analyze the system and understand the areas of improvement.

In process of harvesting algae, system uses magnetic beads to pull algae out of water as mentioned in harvesting methods. To reduce the overall cost of production, it is essential to have optimized systems and processes at every step of biocrude production. Also, there are limitation in optimizing the growth of the algae until some drastic changes occur in biological research. However, harvesting algae is an important step and could take considerable amount of time of overall

production process as mentioned earlier. Hence, hastening this process holds prime importance in biocrude production process. The first step towards optimizing this process is to analyze the fluid flow through the harvester system. Furthermore, the procedure followed for this analysis is equally important to reduce the cost of computational and time. The scope of this thesis is limited to the multiphase flow visualization of water entering into the algae separator system, initially filled with air, and associated flow structures developed into the system. This thesis research does not analyze any magnetic particles in the flow or its effect on the system's efficiency but in general assess various design parameters of the system.

MULTIPHASE FLOW:

In fluid mechanics, multiphase flow refers to different fluid materials that have different interactions with the flow and the potential field in which it is immersed. Multiphase flows can be classified into dispersed and separated flows. In dispersed flows, a continuous phase incorporates the other phase in the form of bubbles, drops or a particulate matter. Separated flows include two or more number of continuous streams of different phases that are separated by interfaces. Both dispersed and separated flows can also be classified based on the type of materials involved in each phase as well as their physical states. In this thesis research, water and air, liquid-gas multiphase, will be the subject of analysis. The type of the multiphase flow determines the required numerical model. Different types of horizontal liquid-gas multiphase flows are as follow:

1. **Stratified or free surface flow:** These flows involve two or more immiscible fluids separated by an interface, e.g. open channel flow, sloshing in moving tank, etc. This type of flow is generally observed at low liquid velocities.
2. **Plug or slug flow:** These flows generally occur due to discrepancies in the concentrations of alternating regions in the flow. Distinguishing factor between plug and slug flows is the

increase in the rate leading to the liquid becomes the dominating phase, e.g. large bubble motion or pressure driven oil flow in pipes.

3. **Bubbly flow:** These flows are created when a discreet continuous bubble formation takes place in the continuous phase of the liquid, e.g. hydraulic jumps, cavitation, etc. this type of flow is generally observed at high liquid velocities.
4. **Annular Flow:** These flows are generated due to the high gas velocities at the central core of the pipe that push the liquid to flow in the near-wall region.
5. **Mist flow:** These flows have the gas phase as the major concentration that carries the liquid.

Free surface flows:

Free surface flows can be found in many hydraulic engineering applications from small water tank filling to large water damp flows where two phases involve mostly water and air, making their study very important. Free surface flow involves many flow structures such as recirculation, vortex formation, flow separation etc. The major driving force in free surface flow is the gravity alone and a typical change in the depth of the flow can be observed along the streamwise direction due to the loss in momentum near the bed caused by the drag. Also, free surface elevation varies when flow encounters bumps or obstacles. When filling a tank, we can observe various flow structure including sloshing movement causing turbulence in the system that varies the free surface structure and introduces air entrainment in the flow field. In the hydraulic jump, free surface breakup and air entrainment can be observed and hence the multiphase model limits can be assessed in such scenarios to capture the free surface deformations. Furthermore, Froude number is of prime importance in multiphase flow which assists in determining the upstream and downstream flow fields behavior depending on the velocity of the fluid. In subcritical flow ($F < 1$) disturbance caused by the obstacle is traveled in both upstream and downstream direction whereas in supercritical flow ($F > 1$), it travels only in downstream direction. For the flows where $F = 1$ the standing wave is

formed in front of the obstacle. Therefore, in free surface flows it is essential to accurately capture free surface elevation. When fluid enters at comparatively still water section energy dissipation becomes a major concern. In current thesis research, the water is pumped into the system and water flows as an effect of both the pump force and gravity.

Multiphase flows characteristics are studied theoretically, numerically, and experimentally in the literature. Computational models provide a low-cost reliable prediction of the flow characteristics. Most common approach to the multiphase problems used by hydraulic engineers is one dimensional (1-D) flow. Some flow scenarios where some aspects of the flow such as velocity, pressure, depth, etc. change with time, called as an unsteady flow, 1-D analysis involves significant attention on longitudinal acceleration, but transverse and vertical accelerations are neglected. When flow parameters are independent of the time, called steady flows, can be uniform or non-uniform flow. Further, flow can be divided into gradually varied and rapidly varied flow. In gradually varied steady flow, flow parameters may change gradually with distance but not with time and have low vertical accelerations. In rapidly varied flow, variations are observed in vertical and/or transverse direction. In unsteady flow, only non-uniform flow is observed, and both gradually varied and rapidly varied flows are possible. In some unsteady problems, approximations are made and considered as a steady flow. These are special cases where a steady flow is observed after a long time of operation. Some of these applications can be solved for steady flow but certain differences are expected as unsteady flow involves certain conditions that are not included in the steady flow governing equations. Increased computational power and improved solvers 1-D unsteady flow was able to predict the hydraulic structures more accurately. Some hydraulic jumps can be solved using 1-D problem but the rapidly varied zone in hydraulic jump must be identified and isolated in the analysis [61]. Furthermore, applications such as filling tank cannot be solved using steady flow as the flow parameters especially the pressure change. Also, some applications such as hydraulic jump

and vortex behind an obstacle involve complex 2-D and/or 3-D flow structures that cannot be accurately solved using 1-D approach. It is required to solve 2-D/3-D governing equations; but, it adds computational cost tremendously [61]. Furthermore, unsteady flow behavior using steady state analysis adds difficulty to capture the fluid accelerations and therefore, it is necessary to consider the structure of the equation governing the particle motion. In CFD, numerous attempts are made using Large Eddy Simulation LES, Improved Delayed Detached Eddy Simulation (IDDES) and hybrid models to solve multiphase problems. Later two models were an attempt to reduce the computational cost of LES. However, these models are still costly and therefore, approximations are introduced by using alone Reynolds Averaged Navier Stokes (RANS) equations to model the flow. Next chapter deals with the modeling of the problem for the analysis and illustrates the method used to solve the problem.

Chapter 3. METHODOLOGY

Figure 7 shows the schematic representation of the system used for this analysis. Water is pumped into the system via the inlet. A steep slope is provided to accelerate the flow due to gravity towards the Algae Collector Disc. This water then reaches to the circular channel section where the collector disc is located. Water starts filling the circular channel section and eventually starts exiting through the outlet of the system. Rotating algae collector disc is a magnetic disc that attracts the magnetic particles immersed in water which has absorbed the microalgae. These attached magnetic particles are finally taken off using scraping mechanism (not shown in the figure). Deflector is provided to redirect the flow towards the algae collector disc and add turbulence to the flow to maximize the capturing rate of algae collector disc.

In this MSc thesis, only one channel with one algae collector disc is analyzed as it represents overall system's configuration and can reflect the same flow feature in each channel. For the sake of simplicity, henceforth algae collector disc is referred as disc. Star CCM+ is used for numerical analysis in this research. An external air chamber is created about the size of the system to incorporate air into the system as this problem represents open channel flow. Sufficient size of the air chamber and proper boundary conditions are required so that less interference of the air flow to the flow of water could be achieved. For this research, following parameters were taken into consideration for analyzing the system:

- Inlet, outlet, and system length dimensions
- Height of the Inlet and outlet to determine the depth of the immersed Magnetic disc in water
- Deflector dimension
- Pump power / inlet condition

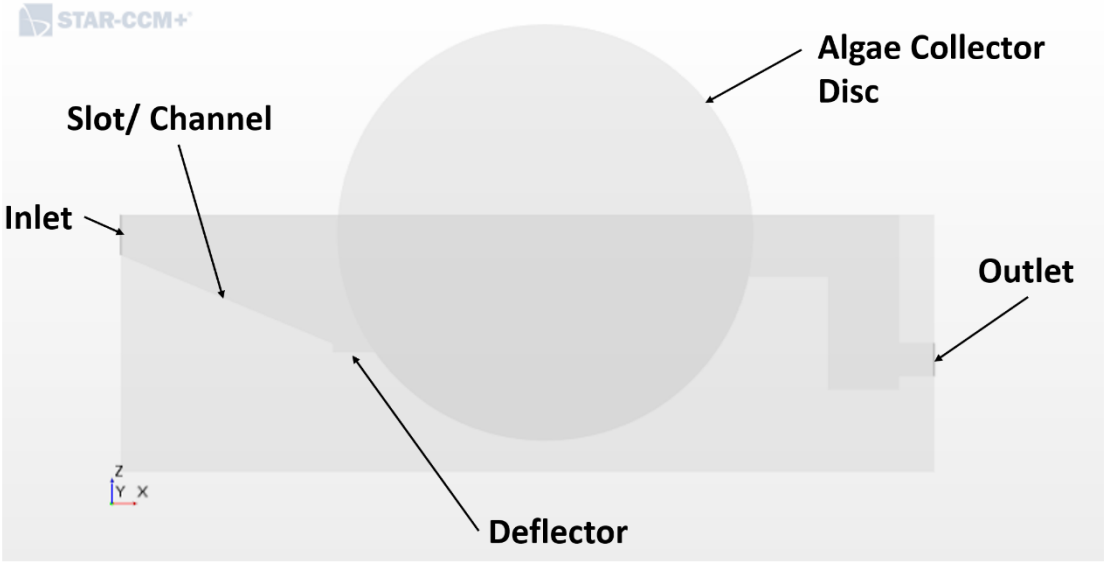

Figure 7 Schematic representation of the system with deflector

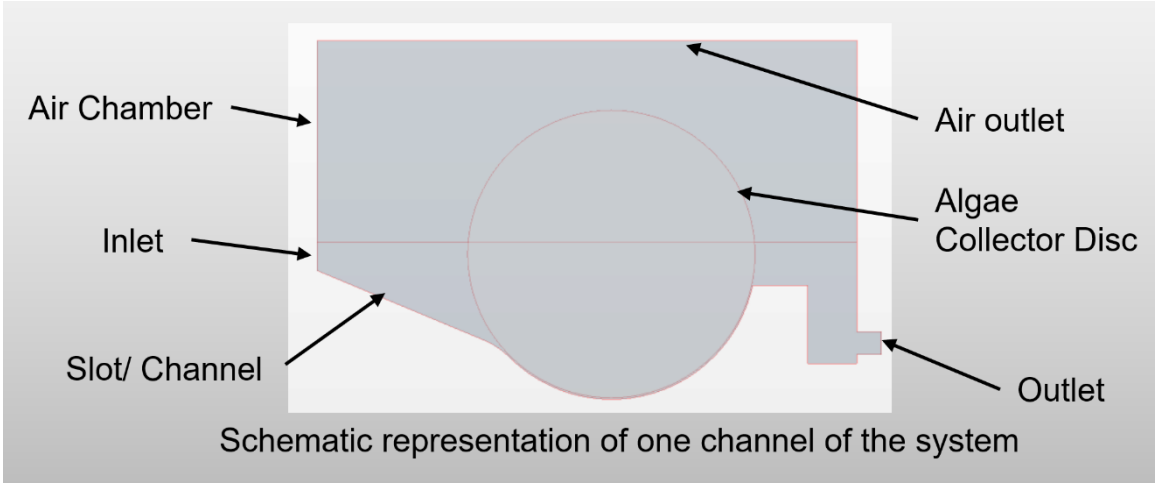

Figure 8 Schematic representation of the system without deflector

NUMERICAL MODEL:

Two main methods are used to solve the multiphase problems and their selection depends on the extent (i.e. fluid particle level) to which the application is exposed to the physics of the problem. Lagrangian Method is used to understand and visualize each particle introduced into the problem and path followed by it. However, this problem does not introduce any particle (Magnetic particle) in the water and not required to visualize the path of each water particle. However, the overall

behavior of the fluid in a control volume and the flow structures are of interest. Therefore, Eulerian numerical method is employed for the multiphase flow analysis and to visualize the flow in a constrained volume of the system. Following Models and Methods were selected:

- Multiphase Eulerian Model
- Volume of Fluid (VOF)
- Finite Volume Method
- Turbulence closure Model
    - K-Epsilon Model (Two layer Realizable $k-\varepsilon$)
    - K- Omega Shear Stress Transport (SST) Model (SST Menter)
- Scheme
    - Steady State
    - Implicit Unsteady

Following are the governing equations solved for CFD analysis**:**

- **Multiphase Eulerian Model**

  In this model, the conservation equations for mass, momentum, and energy are solved

    - Conservation of mass:

$$\frac{\partial \rho}{\partial t} = \nabla \cdot (\rho v) = 0 \tag{1}$$

    - Conservation of momentum:

$$\frac{\partial (\rho v)}{\partial t} + \nabla \cdot (\rho v \times v) = \nabla \cdot \sigma + f_b \tag{2}$$

    - Conservation of energy:

$$\frac{\partial(\rho E)}{\partial t} + \nabla \cdot (\rho E v) = f_b + \nabla \cdot (v \cdot \sigma) + \nabla \cdot q + S_E \quad (3)$$

where, ρ is the density, v is the continuum velocity, f_b is the resultant body forces, σ is stress tensor, q is the heat flux, and S_E is energy source per unit volume

Eulerian Multiphase model resolves the position and shape of the free surface. The VOF offers an efficient way to track the fluid at the interface of air and water using a volume fraction α which helps in determining the variation in depth of the fluid [62]. The value of α varies between 1 and 0 with 1 being region completely occupied by water and 0 by air when solving for water. VOF has shown its ability to accurately measure the flow fields in free surface flows and differs from the Eulerian model for multiphase flow where it solves a single momentum equation on the entire domain making it computationally less expensive.

In Reynolds Averaged Navier Stokes (RANS) equation, turbulence models are used to provide closure to the equation. To obtain the RANS equation, governing equations of mass, momentum equations are averaged, and fluctuating term is added. $\emptyset = \overline{\emptyset} + \emptyset'$ where $\emptyset$ is the instantaneous quantity, $\overline{\emptyset}$ is the averaged quantity and $\emptyset'$ is the fluctuating quantity. These quantities can represent velocity, pressure, and energy. Due to these additional terms, the transport equation can be written as a Reynolds stress tensor:

$$T_t \equiv -\rho \overline{v'v'} = -\rho \begin{pmatrix} \overline{u'u'} & \overline{u'v'} & \overline{u'w'} \\ \overline{u'v'} & \overline{v'v'} & \overline{v'w'} \\ \overline{u'w'} & \overline{v'w'} & \overline{w'w'} \end{pmatrix} \quad (4)$$

- **$k - \varepsilon$ turbulence model:**

In this model, turbulent kinetic energy k and the turbulent dissipation rate ε are defined to calculate the turbulent viscosity for the closure of RANS equations. Realizable $k - \varepsilon$ turbulence model contains new transport equation for the turbulent dissipation rate [63]. In this

model, the critical coefficient is expressed as a function of mean flow and turbulence properties rather than constant values from the standard model. This model offers a higher accuracy and convergence compared to the standard model in many problems. The realizable two-layer $k-\varepsilon$ turbulence model solves with the two-layer approach which adds flexibility of an all y+ wall treatment where ε is prescribed algebraically with distance from the wall in the near wall region where viscosity is dominant. In eddy viscosity model Reynolds Stress Tensor (RST) modeled as a function of mean flow quantities. One way is by Boussinesq approximation as follows:

$$T_t = 2\mu_t S - \frac{2}{3}(\mu_t \nabla \cdot \bar{v} + \rho k) I \tag{5}$$

where, S is the mean strain rate tensor, $\bar{v}$ is the mean velocity, I is the identity tensor. The turbulent viscosity μ_t is computed using following:

$$\mu_t = \rho C_\mu f_\mu k T \tag{6}$$

where, C_μ is a model coefficient, f_μ is a damping function, T is the turbulent time scale.

Following are the realizable $k-\varepsilon$ transport equations [64] of kinetic energy k and turbulent dissipation rate ε:

$$\frac{d}{dt}\int_V (\rho k) dV + \int_A \rho k (v - v_g) \cdot dA = \int_A \left(\mu + \frac{\mu_t}{\sigma_k}\right) \nabla k \cdot dA + \int_V \left[f_c G_k + G_b - \rho\left((\varepsilon - \varepsilon_0) + Y_M\right) + S_k\right] dV \tag{7}$$

$$\frac{d}{dt}\int_V (\rho \varepsilon) dV + \int_A \rho \varepsilon (v - v_g) \cdot dA = \int_A \left(\mu + \frac{\mu_t}{\sigma_\varepsilon}\right) \nabla \varepsilon \cdot dA$$

$$+\int_V \left[f_c C_{\varepsilon_1} S_\varepsilon + \frac{\varepsilon}{k}\left(C_{\varepsilon_1} C_{\varepsilon_3} G_b\right) - \frac{\varepsilon}{k+\sqrt{\nu\varepsilon}} C_{\varepsilon_2}\rho(\varepsilon-\varepsilon_0) + S_\varepsilon\right] dV \qquad (8)$$

where, v and v_g are the mean velocity and reference frame velocity relative to the stationary frame respectively; μ is the dynamic viscosity; σ_k and σ_ε are model coefficients and are 1 and 1.2, respectively; f_c is the curvature correction factor; G_k and G_b are the production terms; ε_0 and T_0 are the ambient turbulence value and specific time scale evaluated at ε_0, respectively; Y_M is the dilatation dissipation; S_k and S_ε are the user-specified source terms; $C_{\varepsilon_1} = \max\left(0.43, \frac{\eta}{5+\eta}\right)$, C_{ε_2} is 1.9 and $C_{\varepsilon_3} = \tanh\frac{|v_b|}{|u_b|}$; u_b and v_b are velocity components perpendicular and parallel to g, respectively. ν is the kinematic viscosity. The equations to find respective terms used to solve transport equations is given in Star CCM+ manual [64]. In this thesis, only realizable $k-\varepsilon$ turbulence model is used and henceforth is only referred as $k-\varepsilon$ for the sake of simplicity.

- **$k-\omega$ turbulence model:**

$k-\omega$ turbulence model is selected for the internal flow analysis to more accurately solve for the flow separation with attachment and detachment of the water at deflector and near the disc area. $k-\varepsilon$ turbulence models including realizable model do not produce accurate enough results when pressure gradient, separation and strong streamline curvatures in the flow are present. This research involves rotating disc and when water is introduced into the system due to strong curvature involved in circular channel section and various attachment and detachment points exists within the disc and circular channel section gap. The $k-\varepsilon$ model was selected for initial setup due to its faster convergence. The results from $k-\varepsilon$ are used for $k-\omega$ model initialization. Furthermore, SST menter k-w model was selected that provides resolved

sensitivity issues with free stream/ inlet conditions by adding cross diffusion term containing dot product of$\Delta\, k \cdot \Delta\omega$ [65].

The SST menter transport equations of kinetic energy k and specific dissipation rate ω are provided in Star CCM+ manual [64] and are as follows:

$$\frac{d}{dt}\int_V (\rho k)dV + \int_A \rho k(v - v_g)\cdot dA = \int_A (\mu + \sigma_k \mu_t)\nabla\, k \cdot dA + \int_V \left[\gamma_{trans}(G_k + G_{nl} + G_k^{\lim} - \gamma'\, \rho\beta^* f_{\beta^*}\, (\omega k - \omega_0 k_0) + S_k\right] dV \quad (9)$$

$$\frac{d}{dt}\int_V (\rho\omega)dV + \int_A \rho\omega(v - v_g)\cdot dA = \int_A (\mu + \sigma_\omega \mu_t)\nabla\, \omega \cdot dA + \int_V (G_\omega - \rho\beta(\omega^2 - \omega_0^2) + D_\omega + S_\omega)\, dV \quad (10)$$

where, γ' and γ_{trans} are the transition model; G_{nl} is the non-linear production term; β is model coefficient; f_{β^*} is the free shear modification factor; k_0 and ω_0 are the ambient turbulence values that counteract turbulence decay [66]; σ_ω is model coefficient; G_ω is the production of specific dissipation rate; D_ω is the cross-derivative term; S_ω are the user-specified source term. The equations to find respective terms used to solve transport equations is given in Star CCM+ manual [64]. In this thesis, only realizable $k - \varepsilon$ turbulence model is used and henceforth is only referred as $k - \varepsilon$ for the sake of simplicity.

The turbulent viscosity $\mu_t$is computed using following:

$$\mu_t = \rho k T \quad (11)$$

COMPUTATIONAL SETUP

For initial setup, steady state scheme without the disc case was used. Analysis of the generated results showed various improvement regions and special attention was provided near the deflector and the vicinity of the section where the water flows during initial stages to reduce initial divergence. To improve mesh various volume sections were generated to improve the mesh size in those regions. Following table illustrates the different mesh configuration used for different cases studied in this MS thesis:

Table 2 Various mesh configuration for without disc case

Mesh parameters	Coarse	Fine	Finer	Very fine
Total Number of cells	0.61 million	0.80 million	1.82 million	1.88 million
Base	8 mm	7 mm	7 mm	5 mm
Number of prism layers	6	8	12	16
Near wall thickness	0.1mm	0.08 mm	0.07 mm	0.02 mm
Total prismatic layer thickness	2.8 mm	2.73 mm	2.73 mm	3 mm

For coarse mesh, 6 number of prism layers with only two control volumes with the mesh size of 35% to the base were applied to capture the flow structures in the circular channel section including deflector and outlet area and made fine compared to other areas. For fine mesh, base size was reduced. Similar volume controls with additional control volume area near inlet was applied in the finer mesh case. Volume control mesh size was reduced to 25% to the base size in the finer mesh. Further additional near wall refinement control volumes were applied in the very fine mesh which included complete inlet and outlet flow areas. Results showed that 0.8 million cases for the without disc case was accurate compared to other and hence comparative study of the without disc case shows only this mesh configuration.

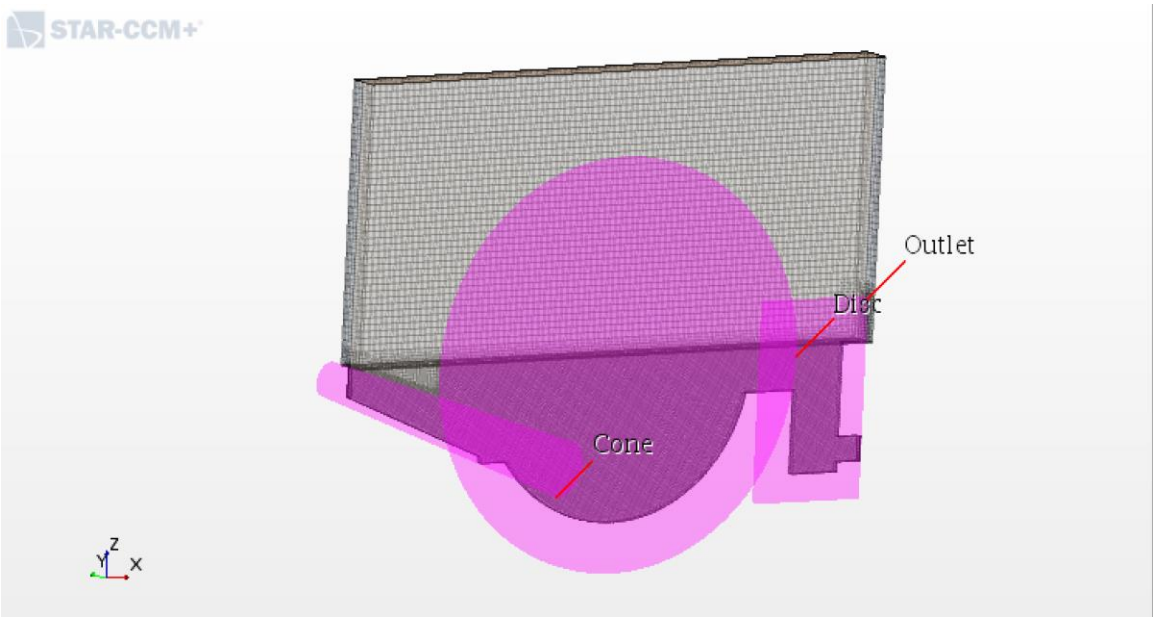

Figure 9 Mesh Improvement for fine mesh without disc case (highlighted geometry shows the volume controls)

Boundary and initial conditions:

No slip boundary conditions were applied on the walls of the system. Mass flow rate as the inlet boundary condition was selected to be 0.1 kg/s. Water distribution of the length 0.4 mm and the thickness equal to the channel cross-sectional thickness and the height of 2 mm above the inlet was added. To facilitate air into the system, top surface of the air chamber was set to pressure outlet boundary condition. For unsteady case, time step of 10^{-3} is used considering the computational power. It was made sure that wall Y+ is less than 5 to accurately capture boundary layer.

Table 3 illustrates various without disc case studied in this MS thesis research with their corresponding mesh configuration and general setup. Steady state has total of four case studies that include grid analysis cases from case 1 to case 3 using $k-\varepsilon$. Case 4 is solved using $k-\omega$ with selected mesh size from grid analysis. Unsteady has one case using $k-\varepsilon$ with selected mesh size from grid analysis.

Table 3 Nomenclature of various case studies and their respective significance

Configuration	Case number	Description
Steady without disc case	Case 1	613725 cells/0.61 million cells $k-\varepsilon$ (45% to base size in Volume Controls)
	Case 2	0.88 million cells $k-\varepsilon$ (7% decrement in cell size in volume controls i.e. 38% to base size)
	Case 3	1.82 million cells $k-\varepsilon$ (reduced base size from 8 mm to 6 mm with keeping the prismatic layer configuration same)
	Case 4	0.88 million cells $k-\omega$ (7% decrement in cell size in volume controls i.e. 38% to base size)
Unsteady without disc case	Case 1	0.88 million cells using $k-\varepsilon$ with increased number of iterations 10 with delta $\Delta T = 10^{-3}$
	Case 2	0.88 million cells using $k-\omega$ with increased number of iterations 10 with delta $\Delta T = 10^{-3}$

CHALLENGES INVOLVED IN SYSTEM MODELING:

Harvester is a floating device and understanding the physics of the system is itself a challenge. The challenge started with implications of the real scenario when the system is at work and confirming its feasibility to replicate during CFD analysis with currently available computational sources. For this research, 24 core processor with 192 GB RAM was used. Further, no similar experimental data was available to determine the accuracy of the results. Therefore, adding complication could make difficult to have a perception of the problem. To simplify it, only one channel with the disc is analyzed rather than the whole system with many number of channels. It was necessary to assume some physical properties to reduce the variables of the problem. First, air chamber was generated, and air outlet conditions were applied on the top of the chamber as well as at the outlet of the system to have a consistent flow of air in and out of the system. Further, steady pump input is assumed at the inlet and with the mass flow rate of 0.1 kg/s to reduce complications of variations in pump input. Constant density and isothermal conditions were applied and hence no temperature variations and their effect on the physics of the system were accounted in this research. Also, it was necessary

to understand the different aspects of the system from design and operating conditions point of view. Therefore, following parameters were assessed in this research:

- Definition of physical scenario (initial conditions)
- Turbulence models and mesh size improvements
- Obtaining uniform flow for given length span of slots

It is important to have a procedure that could effectively assist in the optimization of the system. Also, the procedure should provide results with optimum time and comply with available computational resources. Following is the proposed procedure for analysis of the system:

- **Analyzing flow of a channel without disc**

  For initial intuition of the flow through the system, it is analyzed without the disc which will largely reduce the computational cost and will save the time. At this stage, required necessary changes in the system can be performed and reanalyzed. This will assist in implementing a standard setup for further analysis. Introduction of the disc into the system is very much critical due to the gap between the disc and circular channel section is very small (1.79 mm). A very fine mesh is required in this area. In this study, both steady and unsteady schemes are applied and compared.

- **Analyzing flow with disc**

  Introduction of the disc is a critical step as it involves very small gap in the circular channel section. Disc introduces a bluff body and hence providing a restriction to the flow inducing turbulence in the system This adds stagnation point and flow separation phenomenon into the problem.

- **Analyzing flow with rotating disc**

  Rotating disc involves further complexity to the problem by adding rotational boundary movement in the small gap. It changes flow structures such as recirculation region and especially stagnation point. Various methods are available to analyze rotation depending on the accuracy and computational power. The most common method used is rotating boundary method. Apart from this, rotating reference method and rotating mesh method are also used with later being most expensive for computation which requires considerable attention on mesh between rotating and stationary region on the cost of accuracy. For this research, we are going to use rotating boundary method as it provides both accuracy and less computational power.

- **Optimizing Flow through modifying design parameters**

  After assessment of various design parameters, necessary changes can be made in this step which will include alteration in the design parameters mentioned earlier. These altered parameters can be tested to see the expected changes in flow structures by following previous steps.

Chapter 4. RESULTS

Algae harvesting system without disc was analyzed for both steady and unsteady scheme. In unsteady case, the time for single simulation took almost 120 hours to visualize final stage of operation, when water depth in the circular section is almost constant, making unsteady approach difficult to accept as the ideal method for the analysis at initial stages. Further, a different approach was tried in this research by filling the system to a certain height (height of outlet chamber) as an initial distribution and then initiated the flow into the system. However, this method failed to reduce any simulation time as it takes around the same period to fully develop the flow in the entire system. Also, the development of the flow in the system was observed different than the previous method. Therefore, this method could not be considered as a better approach to the problem. This chapter deals with results of flow field going through the system without disc in general and will compare various turbulence models and scheme used for the analysis.

WITHOUT DISC CASE:

Figure 10 illustrates unsteady analysis using k-ε turbulence model representing the volume fraction of water from when water first entered and reached its maximum height in the recircultion area to the time at which the water exited the system. The time for the fluid to start exiting the system was found around 13 s and around 21 s the system reached its final stage of operation for 0.1 kg/s mass flow rate. Various recirculation vortices were observed near the inlet of circular channel section and in the vicinity of circular channel section. It was observed that near inlet of the circular channel section due to sense of rotation of water will oppose motion of the disc an increased drag could be expected. Also, various turbulent flow stuctures were observed such as mixing of two phases and recirculation regions remained at the entry of the circular channel section even after attainment of final stage of operation indicating turbulent behaviour in this area. Close observation of velocity

vector plot (Figure 11) signified, at circular channel section if the disc was introduced into the system, water will flow against the rotational direction of the disc at the entry. Also, from Figure 11, it can be observed that at the base of the circular channel section, near the outlet area, water flow direction was downwards with high velocity, adding drag for the rotating disc. Maximum velocity of water was found to be around 2 m/s and around 0.3 - 0.6 m/s near the entry and exit of the circular channel section. Most of the area of the circular channel section velocity of water was too low about of the order 10^{-2} to 10^{-4} m/s. At initial filling stage of the circular channel section sloshing movement with various air entrainment was obseved. Various free surface structures with dispersion and variation in the depth of water was observed during this stage (Figure 10).

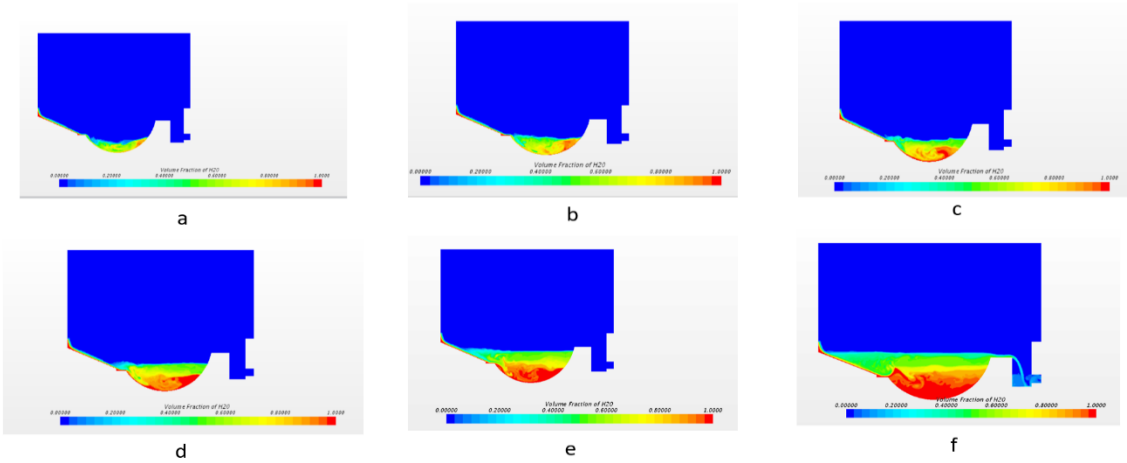

Figure 10 Scalar contours of VOF of water without disc case showing development of the flow in the system

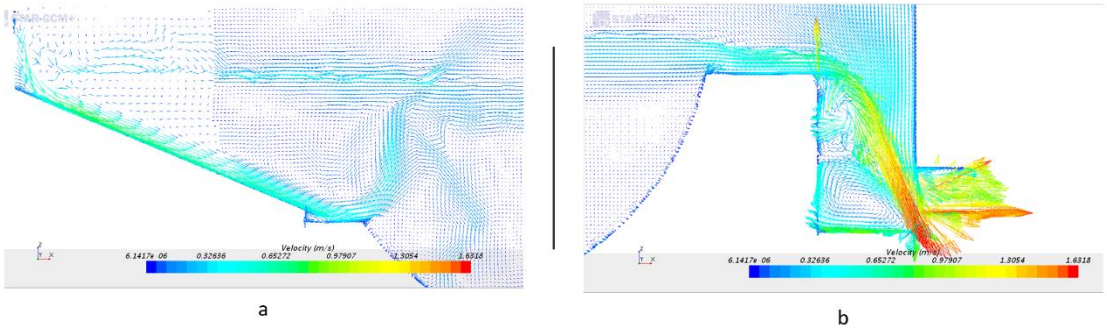

Figure 11 Velocity vector of without disc case (a) Inlet (b) Outlet

EFFECT OF THE DEFLECTOR ON THE FLOW:

Figure 12 and Figure 13 illustrates steady state analysis to observe the effect of the introduction of the deflector into the system and corresponding variation in the flow structure. Velocity vector contours (Figure 12) of with deflector case indicated that this case has a large recirculation near the center of the circular channel section. Downstream of the flow, a jet of water was observed with upward direction at the exit of the deflector. In case of without the deflector, high velocity flow coming from the inlet, flowed further downstream rather than deviated at the deflector and recirculated backwards towards inlet and then upwards and finally merged with incoming free surface flow. In this section, various recirculation regions were observed. Out of these, two were observed near the center bottom of the circular channel section having opposite sense of rotation. Further, due to introduction of deflector in the system, sense of rotation of the flow was reversed than observed in without deflector case.

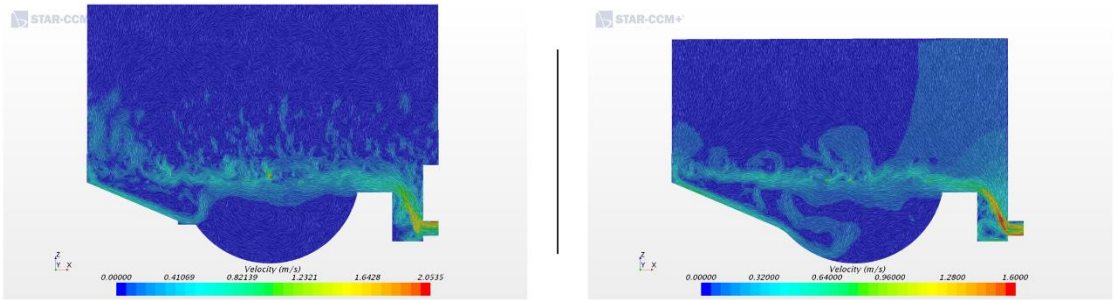

Figure 12 Velocity vector contour of without disc case using k-ε a) with Deflector b) without Deflector

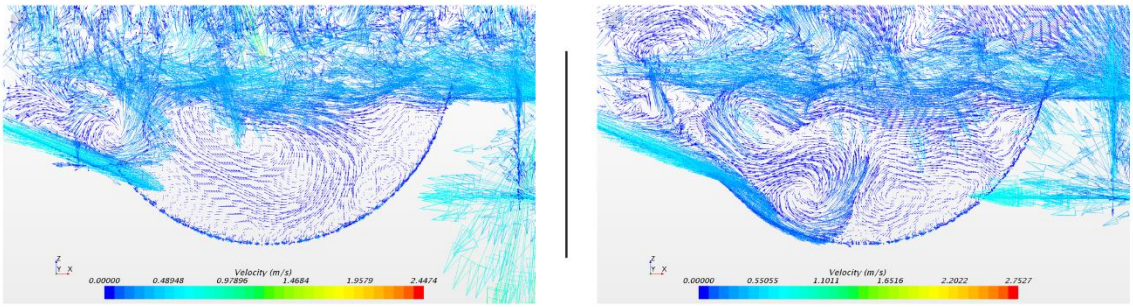

a b

Figure 13 Velocity vector of without disc case using k-ε a) with Deflector b) without Deflector

COMPARATIVE STUDY OF STEADY AND UNSTEADY RANS:

1. Steady without disc case:

Mesh Improvement - Figure 14 to Figure 17 illustrates mesh improvement and its effect on the results when Steady RANS with k−ε turbulence model is employed on without disc. Figure 14 compares VOF contours of case 1 (0.61 million cells) and case 2 (0.8 million cells). Circle is drawn notifying the variation in the results of volume fraction of water. Case 1 failed to predict the volume fraction of water near the slope and inlet area showing lower volume fraction of water due to coarser mesh that caused loss in convection. However, with improved mesh size, volume fraction of water was observed to be more. Further, case 1 reflected more resistance to the incoming flow due to filled water in circular channel section than the case 2.

Grid analysis - mesh size was varied from around 0.61 million cells to 1.8 million cells for the without disc case to analyze effect of the mesh on the results and its convergence. It was found that fine mesh case (0.8 million cells) has shown improved accuracy in the results by reduction in the residuals to 10^{-2} and specifically for momentum equations (10^{-3}). However, no improved results were observed after this case and tend to be diverging the solution. Volume of water of the height of inlet was added with considerable thickness at the inlet to that assisted in proper initialization of the solution. Various thicknesses of water were tried and found water with the little more than

thickness of undeveloped incoming water from inlet provided the convergence and increasing more thickness did not affected the solution afterwards. This effect was also observed in the unsteady analysis. However, effect was found very small as compared to steady analysis.

Velocity vector showed movement of recirculation region in positive x direction and curvilinearly downwards with iteration which originated as smaller recirculation at the inlet side of circular channel section and eventually vanished near the outlet side of the circular channel section. The max velocity was fluctuating from 1.5 m/s to 4 m/s. Furthermore, residuals of steady state illustrated high oscillations in momentum equations reflected system has unsteady flow and unsteady analysis is required to accurately analyze this problem.

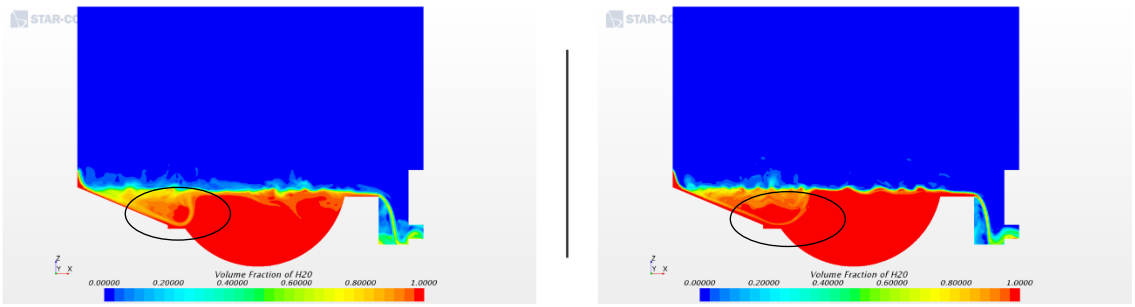

Figure 14 Comparison of mesh improvement on $k-\varepsilon$ turbulence model a)0.61 million cells b) 0.8 million cells

Figure 15 Residuals of 0.6 million cells $k-\varepsilon$ case

Figure 16 Residuals of 0.8 million cells $k-\varepsilon$ case with initial distribution of water near inlet

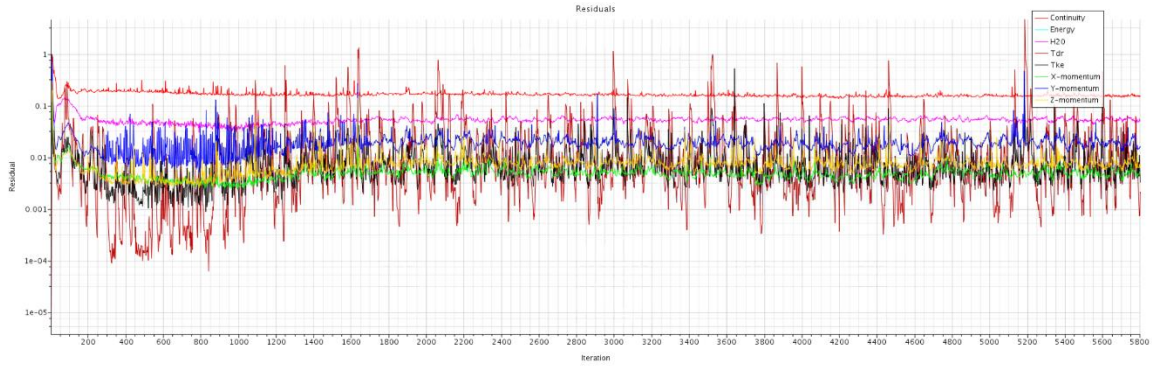

Figure 17 Residuals of 1.8 million cells $k-\varepsilon$ case with initial distribution of water near inlet

2. Effect of turbulence models on the steady scheme:

Figure 18 illustrates the effect of the turbulence model on the flow structures. The $k-\omega$ and $k-\varepsilon$ model has shown similar behavior in the flow. However, certain differences were observed in the circular channel section. Recirculation in the $k-\omega$ model has a sharp curvature with lower radius of curvature as compared to that in the $k-\varepsilon$ and its progression is horizontal as compared to curvilinearly downward of $k-\varepsilon$ indicting unsteady flow and needed to be analyzed using unsteady approach. Further, the size of recirculation region was found to be smaller for $k-\omega$ compared to the $k-\varepsilon$ which was widely spread in circular channel section. Also, momentum equation residuals reduced to the order of 10^{-4} as compared to 10^{-3} in the case of $k-\varepsilon$. However, both $k-\varepsilon$ and $k-\omega$ were close to predict the deflection of the flow at deflector with $k-\omega$ showed greater angle of deflection with z axis. This was the result of sharp recirculation curvature observed in $k-\omega$.

Fluctuations in velocity and pressure profile were observed in both models that indicated the unsteady flow in the system.

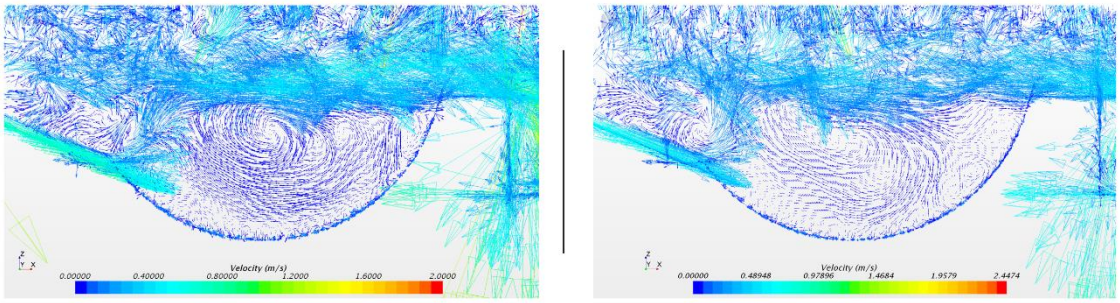

a b

Figure 18 Velocity vector of without disc case (a) k-ω (b) k-ε

3. Unsteady without disc case:

Figure 19 to Figure 23 illustrates comparison between steady and unsteady scheme. For unsteady analysis, simulations were run for 0.8 million case which was observed providing improved accuracy with steady state case. This simulation was run for the physical time of 40 s which required simulation time of 6 days. This made unsteady simulations very expensive. However, unsteady simulation showed improved accuracy with residuals at least in order of 10^{-3} which was 10^{-2} for steady case. Further, accuracy increased by reduction in residuals that were dropped to 10^{-4}. Results showed certain differences in recirculation regions. In unsteady simulation, the core of the recirculation region (Figure 19) was observed at the bottom portion of the circular channel section with comparatively higher velocity at the outer radius of the recirculation region. Also, certain differences were found in unsteady case flow inside the circular channel section than steady case. These differences were observed as a consequence of unsteady flow that affected the steady simulations. However, the direction of rotation of recirculation region using all steady and unsteady cases were in same manner. At outlet section, the jet of the water, as shown in Figure 20, is different for steady and unsteady case. It was found that the mass flow coming into the outlet section is changing with iteration for the steady approach and it was not able to capture recirculation in this

area properly. In unsteady approach, this outlet flow was comparatively continuous with least variation in the recirculation region in outlet section. Furthermore, steady state simulation predicted the wave nature at the water-air interface as higher magnitude waves, whereas in unsteady it remained comparatively constant linear interface from the entrance to the outlet section. Therefore, steady state simulation predicted additional turbulent nature in the flow. The fluctuation in maximum velocity was around 2 m/s which was fluctuating from 1.5 m/s to 4 m/s in steady case. These fluctuations, were mostly observed in outlet section where the water separation was present. It was found outlet section caused reduced accuracy in all the cases when water started entering in outlet section.

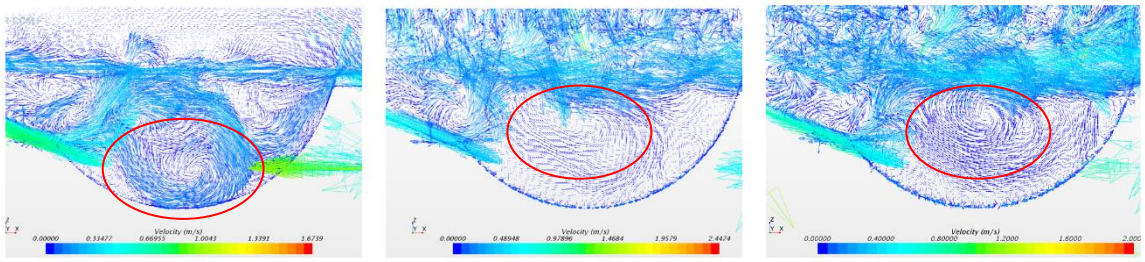

Figure 19 Velocity vector of without disc case a) Unsteady k-ε b) Steady k-ε c) Steady $k-\omega$

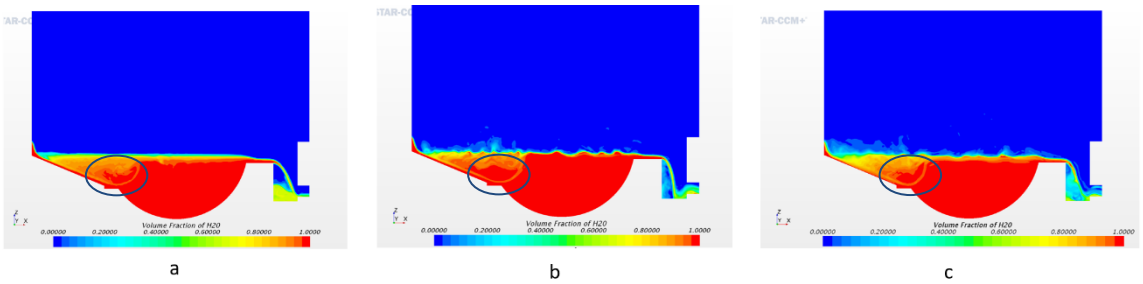

Figure 20 Comparison of VOF of water for without disc case a) Unsteady k-ε b) Steady k-ε c) Steady $k-\omega$

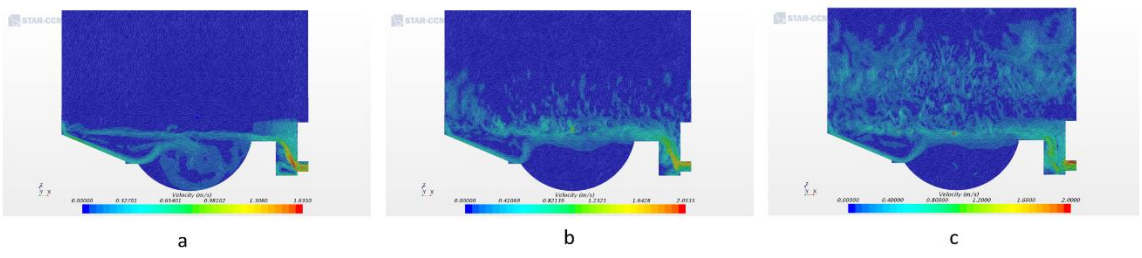

Figure 21 Velocity vector contour of without disc case a) Unsteady k-ε b) Steady k-ε c) Steady k-ω

4. Effect of turbulence models on unsteady scheme:

Figure 22 and Figure 23 illustrates the effect of turbulence model $k-\omega$ on the flow filed using unsteady approach and compared with unsteady and steady $k-\varepsilon$. These comparative studies showed similar trend of convolution of the recirculation region as observed in steady state turbulence model comparison case (Figure 18). In this, the curvature of the recirculation region was more curvilinear having smaller radius of curvature and comparatively smaller in size. In unsteady $k-\omega$ case, location of the core of the recirculation region was found to be around same height as it was observed in unsteady $k-\varepsilon$. Furthermore, angle of the deviated flow found to be similar for both turbulence models using unsteady approach.

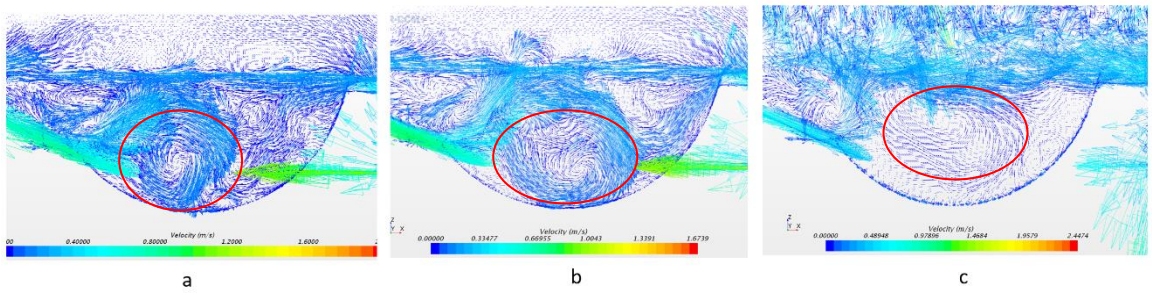

Figure 22 Velocity vector representing effect of turbulence model on the unsteady flow field a) Unsteady k-ω b) Unsteady k-ε c) Steady k-ε

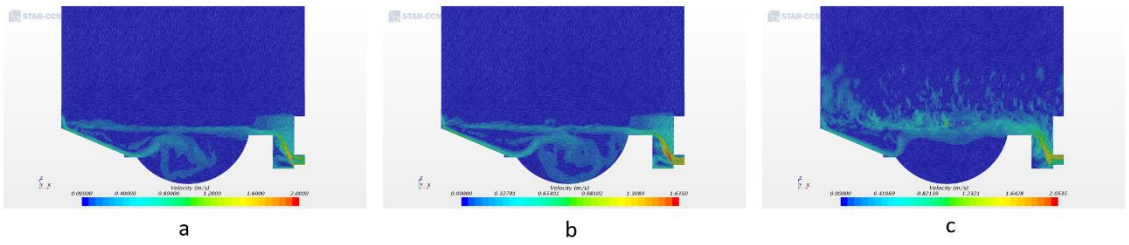

Figure 23 Velocity vector contour representing effect of turbulence model on the unsteady flow field a) Unsteady k-ω b) Unsteady k-ε c) Steady k-ε

Chapter 5. CONCLUSION

Algae harvesting system is an important part of the production of crude oil from algae and it was analyzed for without disc case using steady and unsteady scheme and assessment was performed on various design and operating parameters. Results of velocity and volume fraction of water were plotted to observe overall behavior in the system. The time for the fluid to first exit the system was found around 13 s and around 21 s the system was at its final stage of operation.

Steady state analysis was necessary as it required minimum time for each simulation to provide brief introduction of the flow into the system that assisted in required intuition of the flow through the system. However, it can be concluded that steady approach has inherent inaccuracies in measuring flow structure as the flow in the system was observed to be unsteady. Use of initial distribution of water near the inlet area reduced the initial inaccuracies and further divergence in both unsteady and steady approach and hence improved overall accuracy of the results. Conclusion was made to use small amount of initial distribution of water near the inlet area covering the inlet could assist in proper initialization of simulation. Turbulence model has shown differences in flow structures and found to be providing similar trend of curvilinearity of the recirculation regions when compared with steady and unsteady approach. In unsteady analysis, certain differences were observed in the flow structures than the steady state simulations therefore it is required the flow structures to be analyzed using experimental analysis. Further, unsteady analysis lead to increased analysis time. Due to limitation in time, only unsteady simulation of the without disc case was performed using both turbulence model. However, for with disc case, it will take considerable amount of time due to finer mesh requirement near the disc area where very small gap of about 1.79 mm is present, further making analysis computationally costly. Therefore, the described analysis procedure is effective in all respects providing best possible results in least amount of time and will improve overall optimization procedure.

Deflector was found to be an important feature to direct the flow around the disc and it is a key factor that can generate considerable changes in flow structures inside the circular channel section. Direction of the deflected water at deflector can determine the accuracy of the structure inside the circular section. Therefore, accurate prediction of this angle could provide accurate results. Analysis of the flow without disc case showed combined effect of recircualtion areas and opposition to the rotaiton of disc of water in the vicinity of circular channel section can demand increased power for the disc rotaion. Velocity profile indicated that at circular channel section the water at the base of the cross section will likely to remain stationary and hardly will participate to recirculate to the pond through the exit. Only water on the upper surface and the water deviated due to deflector likely to take major participation to recirculate to the river from the system. Further, changing the angle of deflector to obtain the flow towards outlet section could reduce both the drag and will accelerate the flow towards the outlet. Other way to achieve the same may be to accelerate the flow by either increasing pumping pressure and hence mass flow rate, or by increasing the height of the inlet to have steeper slope before the circular section that will reduce vertical velocity of the fluid at deflector. The ideal case would be horizontal flow at the deflector and reduce the height of the outlet to the height of deflector to achieve minimum depth of water in circular cross-section and accelerate the flow out of the system. This will reduce the time of operation. Also, it will reduce the back flow upstream to the entry of the circular section that minimizes amount of water interacting with the rotating disc. However, for successful application to capture all the magnetic particles it is required to provide the time to interact the water with rotating disc. This will increase the time of operation but will enhance the efficiency of the system. However, it totally depends on the magnetic disc size, its rotational speed, gap between the disc and the wall of the system and direction and velocity of the water at circular channel section.

This research only focused on the water flow into the system without disc case and further analysis is required for with disc case. Also, experimental analysis is needed to validate the result and to concluded which method provides the best results. Further, no magnetic particles with algae were introduced or its movement in the magnetic field of rotating magnetic disc is analyzed. Thereby, providing opening for further research on the flow analysis and particle introduction into the analysis. Lagrangian multiphase can be used to analyze flow of the magnetic particles into the water flow. Also, magnetism effect on the particle flow and finally its effect on the previous simulations is required. Additionally, effects of variation in temperature, fluid film formation and variation in operating parameters should be considered.

REFERENCES

1. *Oil and Petroleum Products* 2017; Available from: https://www.eia.gov/Energyexplained/index.cfm?page=oil_home.

2. *Petroleum & Other Liquids*. February 7, 2018; Available from: https://www.eia.gov/petroleum/weekly/archive/2018/180207/includes/analysis_print.php.

3. *Oil and the Environment*. 2017 February 1, 2017; Available from: https://www.eia.gov/Energyexplained/index.cfm?page=oil_environment.

4. Drew Griffin, N.B.a.C.D., *5 years after the Gulf oil spill: What we do (and don't) know*. April 20, 2015, CNN.

5. *Keystone Pipeline leaks 210,000 gallons of oil in South Dakota*. November 16th, 2017, FOX News.

6. Parker, M.S., T. Mock, and E.V. Armbrust, *Genomic insights into marine microalgae.* Annual review of genetics, 2008. **42**: p. 619-645.

7. Mata, T.M., A.A. Martins, and N.S. Caetano, *Microalgae for biodiesel production and other applications: a review.* Renewable and sustainable energy reviews, 2010. **14**(1): p. 217-232.

8. Spolaore, P., et al., *Commercial applications of microalgae.* Journal of bioscience and bioengineering, 2006. **101**(2): p. 87-96.

9. Varshney, P., et al., *Extremophilic micro-algae and their potential contribution in biotechnology.* Bioresource technology, 2015. **184**: p. 363-372.

10. Sudhakar, M., et al., *Biosaccharification and ethanol production from spent seaweed biomass using marine bacteria and yeast.* Renewable Energy, 2017. **105**: p. 133-139.

11. Xu, M., M. Bernards, and Z. Hu, *Algae-facilitated chemical phosphorus removal during high-density Chlorella emersonii cultivation in a membrane bioreactor.* Bioresource technology, 2014. **153**: p. 383-387.

12. Golueke, C.G., W.J. Oswald, and H.B. Gotaas, *Anaerobic digestion of algae.* Applied microbiology, 1957. **5**(1): p. 47.

13. Demirbas, A. and M.F. Demirbas, *Importance of algae oil as a source of biodiesel.* Energy conversion and management, 2011. **52**(1): p. 163-170.

14. Nhat, P.V.H., et al., *Can algae-based technologies be an affordable green process for biofuel production and wastewater remediation?* Bioresource technology, 2018.

15. Ruiz, J., et al., *Towards industrial products from microalgae.* Energy & Environmental Science, 2016. **9**(10): p. 3036-3043.

16. Gambelli, D., et al., *Third generation algae biofuels in Italy by 2030: A scenario analysis using Bayesian networks.* Energy Policy, 2017. **103**: p. 165-178.

17. Chisti, Y., *Biodiesel from microalgae Biotechnology Advances 25: 294–306.* Google Scholar, 2007.

18. Singh, R., B. Balagurumurthy, and T. Bhaskar, *Hydrothermal liquefaction of macro algae: effect of feedstock composition.* Fuel, 2015. **146**: p. 69-74.

19. Christenson, L. and R. Sims, *Production and harvesting of microalgae for wastewater treatment, biofuels, and bioproducts.* Biotechnology advances, 2011. **29**(6): p. 686-702.

20. Brennan, L. and P. Owende, *Biofuels from microalgae—a review of technologies for production, processing, and extractions of biofuels and co-products.* Renewable and sustainable energy reviews, 2010. **14**(2): p. 557-577.

21. Sing, S.F., et al., *Production of biofuels from microalgae.* Mitigation and adaptation strategies for global change, 2013. **18**(1): p. 47-72.

22. Shen, Y., et al., *Microalgae mass production methods.* Transactions of the ASABE, 2009. **52**(4): p. 1275-1287.

23. Ho, S.-H., et al., *Perspectives on microalgal CO2-emission mitigation systems—a review.* Biotechnology advances, 2011. **29**(2): p. 189-198.

24. Darzins, A., P. Pienkos, and L. Edye, *Current status and potential for algal biofuels production.* A report to IEA Bioenergy Task, 2010. **39**.

25. Shukla, S.K., et al., *Critical evaluation of algal biofuel production processes using wastewater*, in *Algal Biofuels*. 2017, Springer. p. 189-225.

26. Kebede-Westhead, E., C. Pizarro, and W.W. Mulbry, *Treatment of swine manure effluent using freshwater algae: production, nutrient recovery, and elemental composition of algal biomass at four effluent loading rates.* Journal of applied phycology, 2006. **18**(1): p. 41-46.

27. Johnson, M.B. and Z. Wen, *Development of an attached microalgal growth system for biofuel production.* Applied microbiology and biotechnology, 2010. **85**(3): p. 525-534.

28. Katarzyna, L., G. Sai, and O.A. Singh, *Non-enclosure methods for non-suspended microalgae cultivation: literature review and research needs.* Renewable and Sustainable Energy Reviews, 2015. **42**: p. 1418-1427.

29. Gupta, R.B. and A. Demirbas, *Gasoline, diesel, and ethanol biofuels from grasses and plants*. 2010: Cambridge University Press.

30. Mathur, M., A. Bhattacharya, and A. Malik, *Advancements in Algal Harvesting Techniques for Biofuel Production*, in *Algal Biofuels*. 2017, Springer. p. 227-245.

31. Tian, C., et al., *Hydrothermal liquefaction for algal biorefinery: a critical review.* Renewable and Sustainable Energy Reviews, 2014. **38**: p. 933-950.

32. Ghadiryanfar, M., et al., *A review of macroalgae production, with potential applications in biofuels and bioenergy.* Renewable and Sustainable Energy Reviews, 2016. **54**: p. 473-481.

33. Reddy, H.K., et al., *Subcritical water extraction of lipids from wet algae for biodiesel production.* Fuel, 2014. **133**: p. 73-81.

34. Shakya, R., et al., *Effect of temperature and Na 2 CO 3 catalyst on hydrothermal liquefaction of algae.* Algal Research, 2015. **12**: p. 80-90.

35. Tommaso, G., et al., *Chemical characterization and anaerobic biodegradability of hydrothermal liquefaction aqueous products from mixed-culture wastewater algae.* Bioresource technology, 2015. **178**: p. 139-146.

36. Maddi, B., et al., *Quantitative characterization of the aqueous fraction from hydrothermal liquefaction of algae.* Biomass and Bioenergy, 2016. **93**: p. 122-130.

37. Shanmugam, S.R., S. Adhikari, and R. Shakya, *Nutrient removal and energy production from aqueous phase of bio-oil generated via hydrothermal liquefaction of algae.* Bioresource technology, 2017. **230**: p. 43-48.

38. Tian, C., Z. Liu, and Y. Zhang, *Hydrothermal Liquefaction (HTL): A Promising Pathway for Biorefinery of Algae*, in *Algal Biofuels*. 2017, Springer. p. 361-391.

39. Yang, X., et al., *Carbon distribution of algae-based alternative aviation fuel obtained by different pathways.* Renewable and Sustainable Energy Reviews, 2016. **54**: p. 1129-1147.

40. Liu, X., et al., *Pilot-scale data provide enhanced estimates of the life cycle energy and emissions profile of algae biofuels produced via hydrothermal liquefaction.* Bioresource technology, 2013. **148**: p. 163-171.

41. Cerón, M.C., et al., *Recovery of lutein from microalgae biomass: development of a process for Scenedesmus almeriensis biomass.* Journal of agricultural and food chemistry, 2008. **56**(24): p. 11761-11766.

42. Roesijadi, G., et al., *Macroalgae as a biomass feedstock: a preliminary analysis*. 2010, Pacific Northwest National Laboratory (PNNL), Richland, WA (US).

43. Lam, M.K. and K.T. Lee, *Microalgae biofuels: a critical review of issues, problems and the way forward.* Biotechnology advances, 2012. **30**(3): p. 673-690.

44. Pittman, J.K., A.P. Dean, and O. Osundeko, *The potential of sustainable algal biofuel production using wastewater resources.* Bioresource technology, 2011. **102**(1): p. 17-25.

45. Van Ierland, E. and L. Peperzak, *Separation of marine seston and density determination of marine diatoms by density gradient centrifugation.* Journal of plankton research, 1984. **6**(1): p. 29-44.

46. Edzwald, J., *Algae, bubbles, coagulants, and dissolved air flotation.* Water Science and Technology, 1993. **27**(10): p. 67-81.

47. Granados, M., et al., *Evaluation of flocculants for the recovery of freshwater microalgae.* Bioresource technology, 2012. **118**: p. 102-110.

48. Murphy, C.F. and D.T. Allen, *Energy-water nexus for mass cultivation of algae.* environmental science & technology, 2011. **45**(13): p. 5861-5868.

49. Grima, E.M., et al., *Recovery of microalgal biomass and metabolites: process options and economics.* Biotechnology advances, 2003. **20**(7-8): p. 491-515.

50. Udom, I., et al., *Harvesting microalgae grown on wastewater.* Bioresource technology, 2013. **139**: p. 101-106.

51. Shelef, G., A. Sukenik, and M. Green, *Microalgae harvesting and processing: a literature review*. 1984, Technion Research and Development Foundation Ltd., Haifa (Israel).

52. Uduman, N., et al., *Dewatering of microalgal cultures: a major bottleneck to algae-based fuels.* Journal of renewable and sustainable energy, 2010. **2**(1): p. 012701.

53. Zhou, W., et al., *Environment-enhancing algal biofuel production using wastewaters.* Renewable and sustainable energy reviews, 2014. **36**: p. 256-269.

54. Kligerman, D.C. and E.J. Bouwer, *Prospects for biodiesel production from algae-based wastewater treatment in Brazil: A review.* Renewable and Sustainable Energy Reviews, 2015. **52**: p. 1834-1846.

55. Hu, Y.-R., et al., *Efficient harvesting of marine microalgae Nannochloropsis maritima using magnetic nanoparticles.* Bioresource technology, 2013. **138**: p. 387-390.

56. Xu, L., et al., *A simple and rapid harvesting method for microalgae by in situ magnetic separation.* Bioresource technology, 2011. **102**(21): p. 10047-10051.

57. Cerff, M., et al., *Harvesting fresh water and marine algae by magnetic separation: screening of separation parameters and high gradient magnetic filtration.* Bioresource technology, 2012. **118**: p. 289-295.

58. Prochazkova, G., et al., *Physicochemical approach to freshwater microalgae harvesting with magnetic particles.* Colloids and Surfaces B: Biointerfaces, 2013. **112**: p. 213-218.

59. Hu, Y.-R., et al., *A magnetic separator for efficient microalgae harvesting.* Bioresource technology, 2014. **158**: p. 388-391.

60. Wang, S.-K., et al., *Harvesting microalgae by magnetic separation: a review.* Algal Research, 2015. **9**: p. 178-185.

61. Franz, D.D. and C.S. Melching, *Full Equations (FEQ) model for the solution of the full, dynamic equations of motion for one-dimensional unsteady flow in open channels and through control structures*. 1997: US Department of the Interior, US Geological Survey.

62. Hirt, C.W. and B.D. Nichols, *Volume of fluid (VOF) method for the dynamics of free boundaries.* Journal of computational physics, 1981. **39**(1): p. 201-225.

63. Shih, T.-H., et al., *A new k-ϵ eddy viscosity model for high reynolds number turbulent flows.* Computers & Fluids, 1995. **24**(3): p. 227-238.

64. Siemens, *Star CCM+ user manual*. 2016: Siemens.

65. Menter, F.R., *Two-equation eddy-viscosity turbulence models for engineering applications.* AIAA journal, 1994. **32**(8): p. 1598-1605.

66. Spalart, P.R. and C.L. Rumsey, *Effective inflow conditions for turbulence models in aerodynamic calculations.* AIAA journal, 2007. **45**(10): p. 2544-2553.